Synthesis of Composition and Size Controlled AuAg Alloy Nanocrystals via Fe^{2+}-assisted Citrate Reduction

Yujiao Xiahou[a], Yijing Li[a], Peina Zhang[a], Lihui Huang[b], Dayang Wang[c] and Haibing Xia*[a]

[a]State Key Laboratory of Crystal Materials, Shandong University, Jinan, 250100, P. R China.

[b]School of Environmental Science and Engineering, Shandong University, Jinan, 250100, P. R China.

[c]Department of Civil, Environmental and Chemical Engineering, School of Engineering, RMIT University, Melbourne, VIC 3001, Australia.

Figure S1. TEM images (a to c) and extinction spectra (d) of AuAg NCs obtained under diffident concentrations of Au^{3+}: 0.013 mM (a, black curve), 0.019 mM (b, red curve), and 0.056 mM (c, blue curve). The concentrations of citrate and Ag^{+} used in the reaction solution are 0.69 and 0.297 mM. The ratios of Fe^{2+} to Au^{3+} are always 0.03. The extinction curve (magenta curve) of 46 nm CS AuAg ANCs was also shown for better comparison.

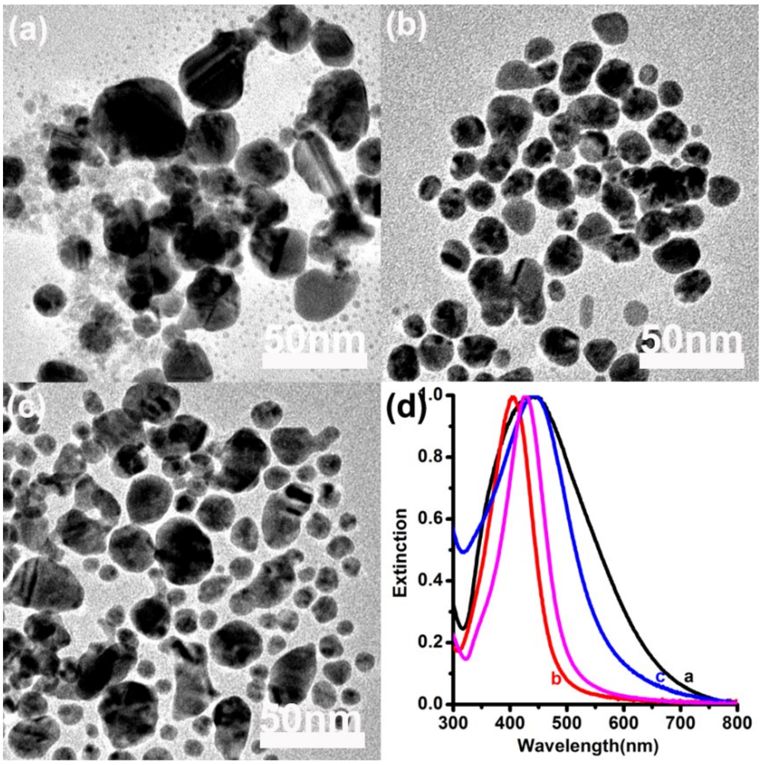

Figure S2. Extinction spectra of the dispersion of 11 nm AuAg ANCs (a), 9.9 nm Au NCs (b) and the solution of pure $FeSO_4$ (c).

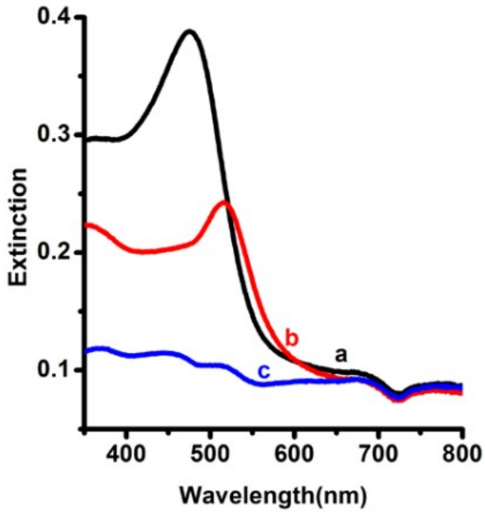

Figure S3. Point-by-point STEM-EDS results (point 1 to 4) of content changes of Au and Ag from the center to outer part of the 25 nm AuAg ANCs. The point 1 located at the center of the 25 nm AuAg ANCs (yellow region), the point 2 located the parts close to center (region enclosed by red line), the point 3 located at the parts close to edge (region enclosed by green line), and the point 4 located at the outermost edge part (region enclosed by blue line).

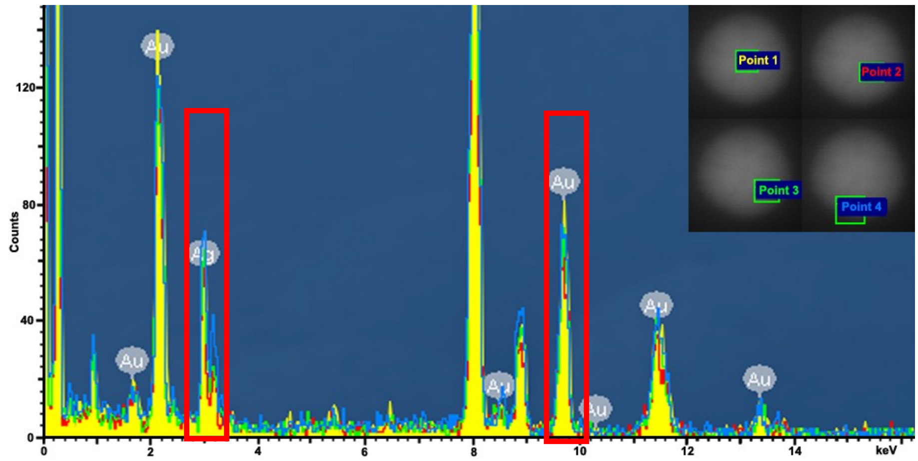

	Point 1	Point 2	Point 3	Point 4
Au (9.7 keV)/cts	82	76	74	72
Ag (3.0 keV)/cts	52	56	64	72

Figure S4. TEM images of the resulting 25 nm AuAg ANCs after stability test of 24 h by a mixed solution containing 0.5 wt% PVP, 0.5 M H_2O_2, and 0.4 M $NH_3{\cdot}H_2O$.

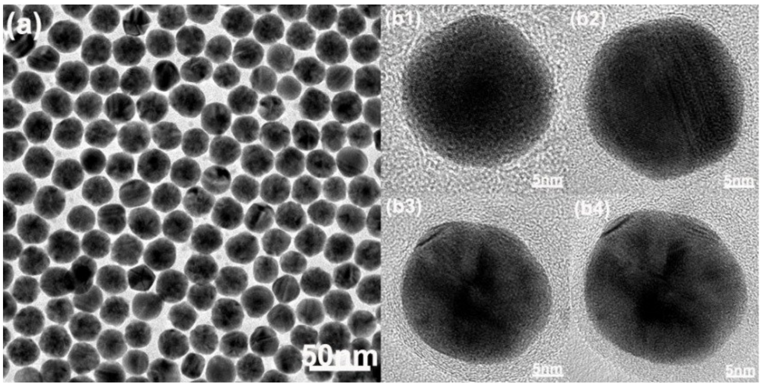

Figure S5. Point-by-point STEM-EDS results (point 1 to 4) of content changes of Au and Ag from the center to outer part of 46 nm CS AuAg ANCs. The point 1 located at the center of 46 nm CS AuAg ANCs (yellow region), the point 2 located the parts close to center (region enclosed by red line), the point 3 located at the parts close to edge (region enclosed by green line), and the point 4 located at the outermost edge part (region enclosed by blue line).

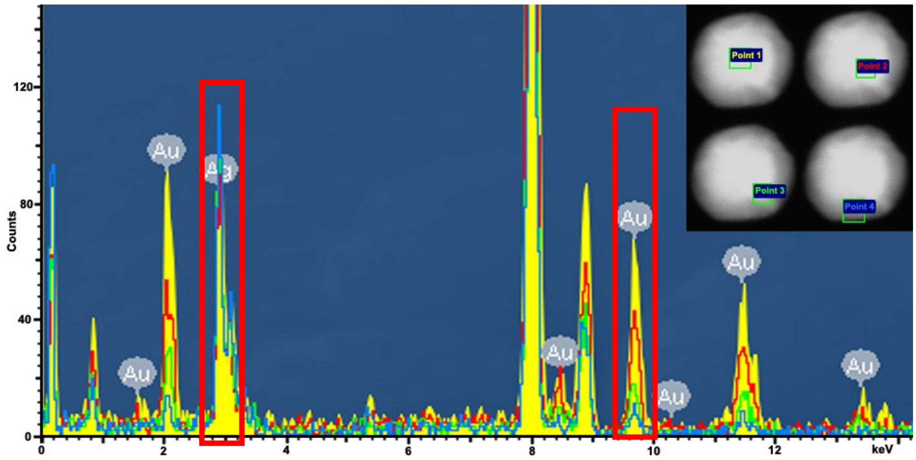

	Point 1	Point 2	Point 3	Point 4
Au (9.7 keV)/cts	70	42	17	12
Ag (3.0 keV)/cts	76	90	96	112

Figure S6. Point-by-point STEM-EDS results (point 1 to 4) of content changes of Au and Ag from the center to outer part of 80 nm CS AuAg ANCs. The point 1 located at the center of 80 nm CS AuAg ANCs (yellow region), the point 2 located the parts close to center (region enclosed by red line), the point 3 located at the parts close to edge (region enclosed by green line), and the point 4 located at the outermost edge part (region enclosed by blue line).

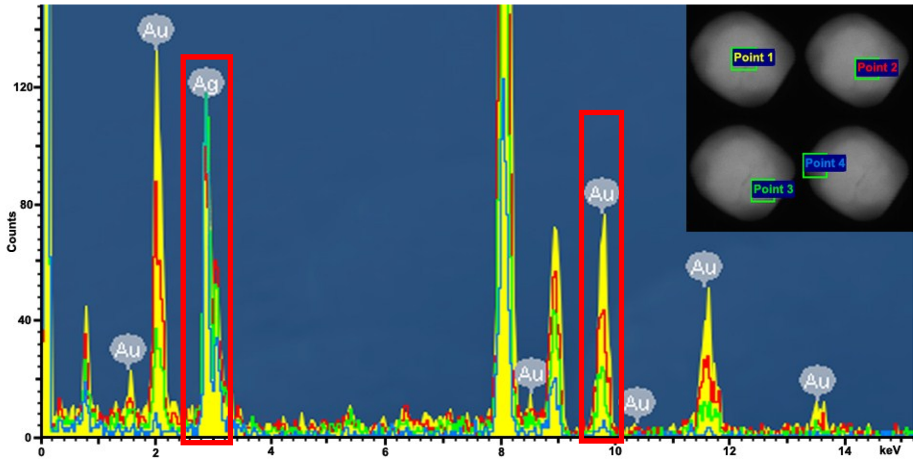

	Point 1	Point 2	Point 3	Point 4
Au (9.7 keV)/cts	76	42	24	6
Ag (3.0 keV)/cts	88	100	110	118

Figure S7. TEM images of the resulting 46 nm CS AuAg ANCs after stability test of 24 h by a mixed solution containing 0.5 wt% PVP, 0.5 M H_2O_2 and 0.4 M $NH_3{\cdot}H_2O$.

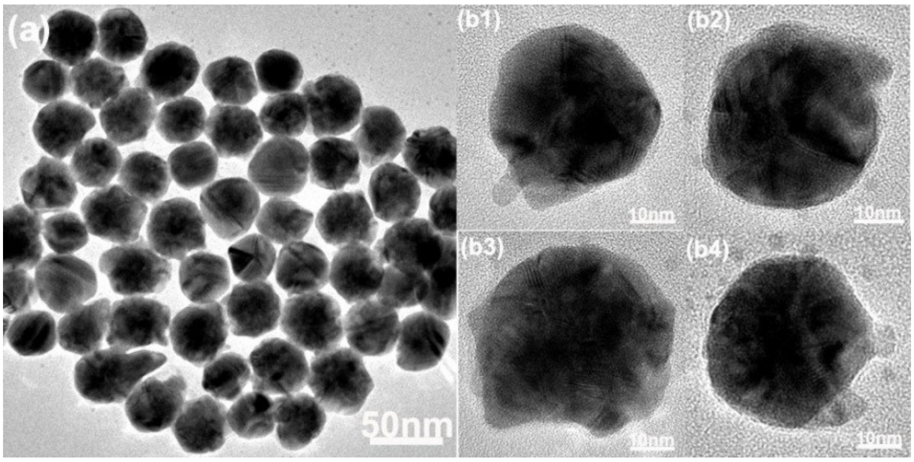

Figure S8. TEM images of the resulting 80 nm CS AuAg ANCs after stability test of 24 h by a mixed solution containing 0.5 wt% PVP, 0.5 M H_2O_2 and 0.4 M $NH_3{\cdot}H_2O$.

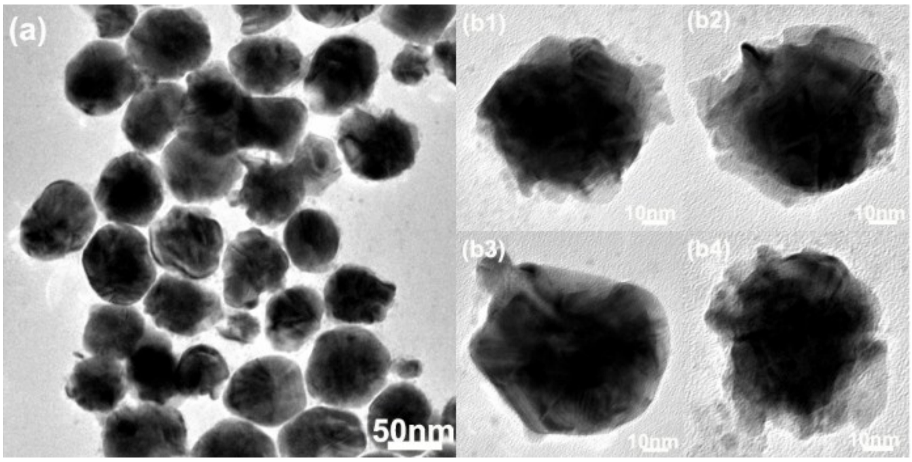

Figure S9. XRD patterns of 46 nm CS AuAg ANCs (red curve) and 25 nm AuAg ANCs (blue curve).

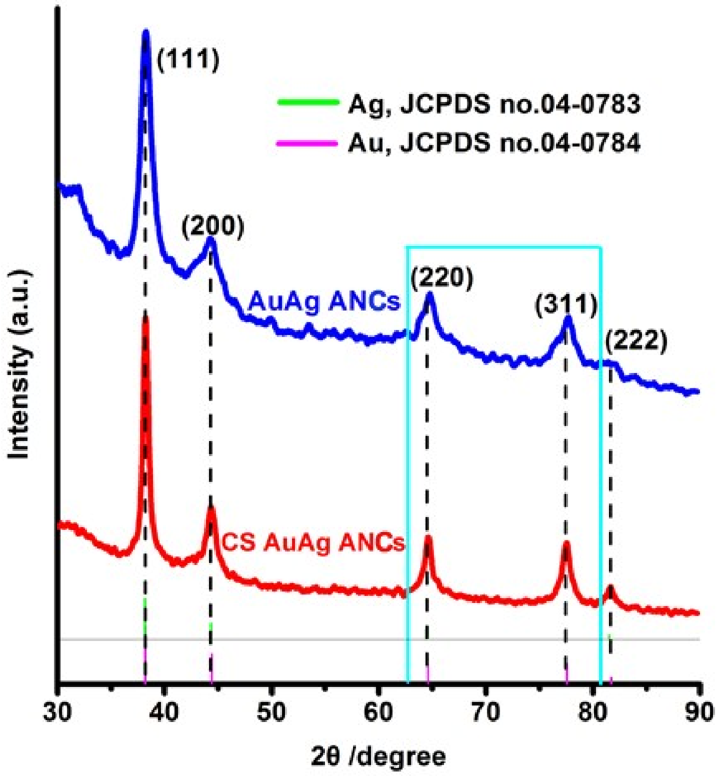

Figure S10. High angle annular dark field—scanning transmission electron microscope—energy dispersive spectrometer (HAADF-STEM-EDS) mapping images and their overlapped image (a to k) of intermediate products of 25 nm AuAg ANCs recorded at different reaction time: 10 s (a), 20s (b) 30 s (c), 60s (d), 120 s (e), 180 s (f), 240 s (g), 300 s (h), 360 s (i), 480 s (j), and 600 s (k).

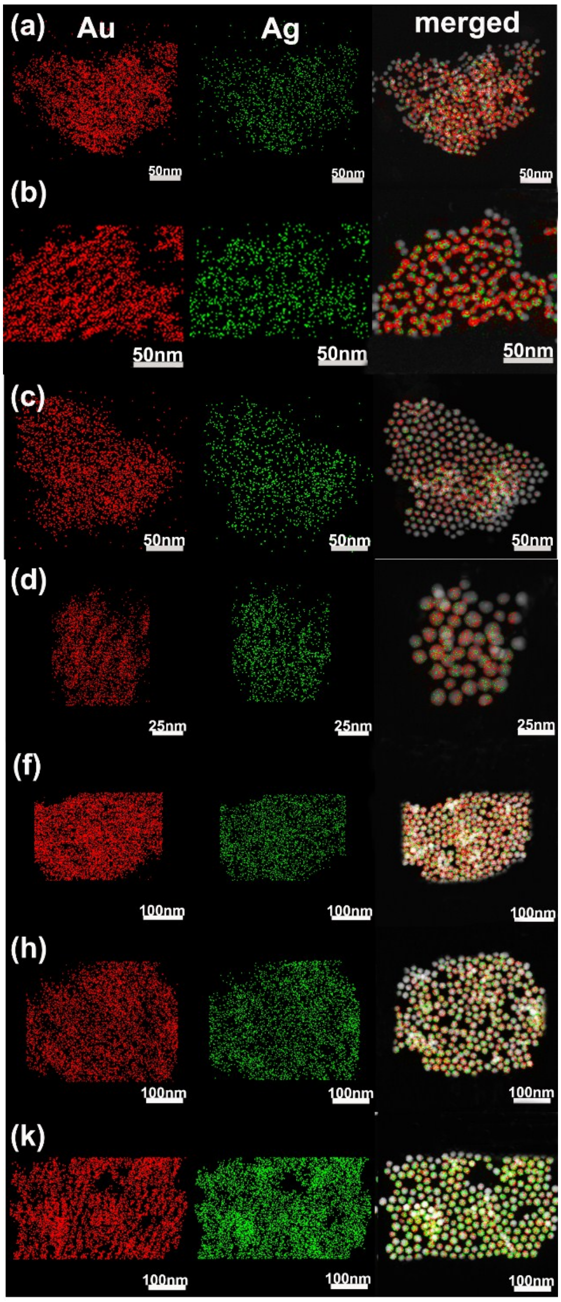

Figure S11. Normal Raman spectrum of the neat film of 4-ATP molecules. The excitation laser wavelength for Raman measurements is 633 nm. The acquisition time is 10 s.

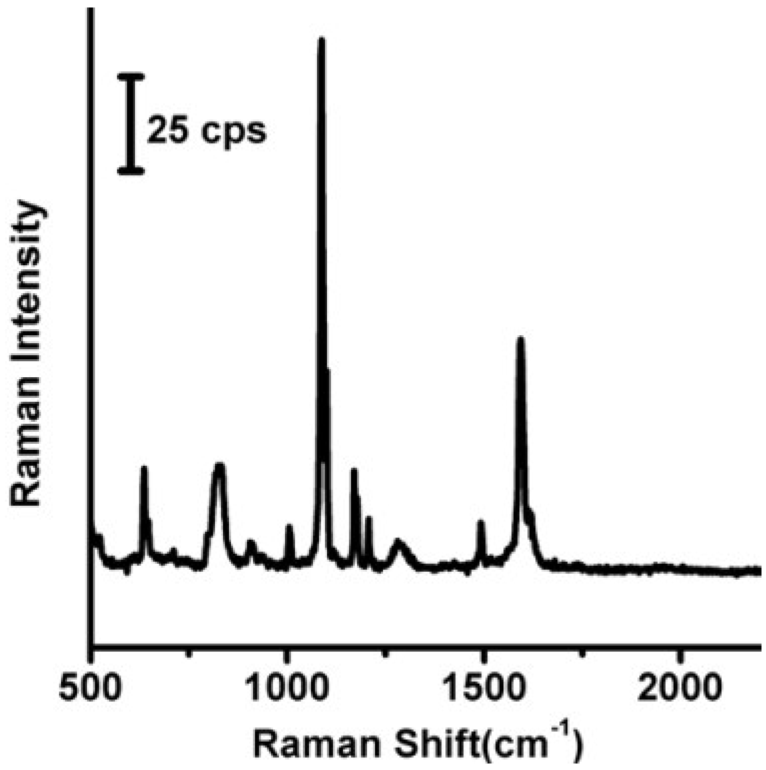

Figure S12. Extinction spectra of as-prepared AuAg ANCs (a to c) and CS AuAg ANCs (d to g) before (black curve) and after (red curve) the stability testing. The sizes of the resulting NCs were 11 nm (a), 16 nm (b), 25 nm (c), 30 nm (d), 46 nm (e), 64 nm (f), and 80 nm (g), respectively.

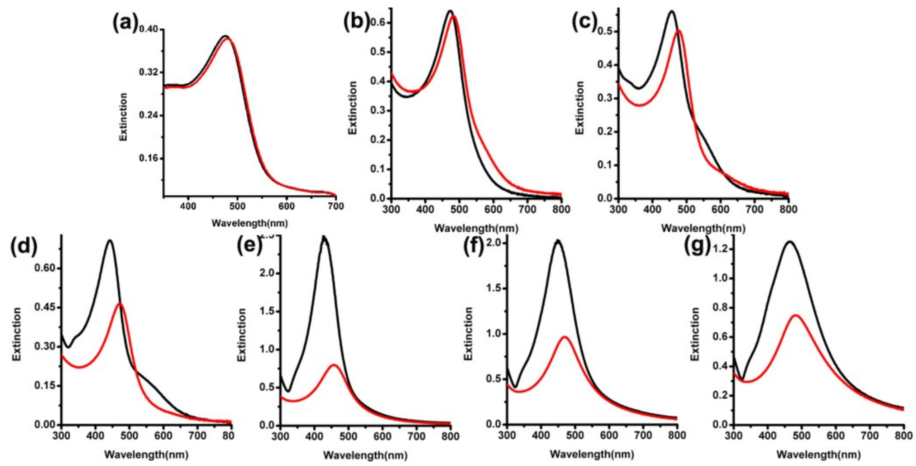

Figure S13. SERS spectra of benzidine (0.50 μM) in an artificial industrial wastewater (2 wt % NaCl, 1 mM H_2O_2, pH 10) absorbed on the aggregates of 25 nm AuAg ANCs on the glass substrates by soaking correspondingly pre-prepared substrates in the wastewater for 10 min (black curve), 1 h (red curve), 6 h (blue curve) and 24 h (magenta curve). The excitation laser wavelength for Raman measurements is 633 nm. The acquisition time is 2 s.

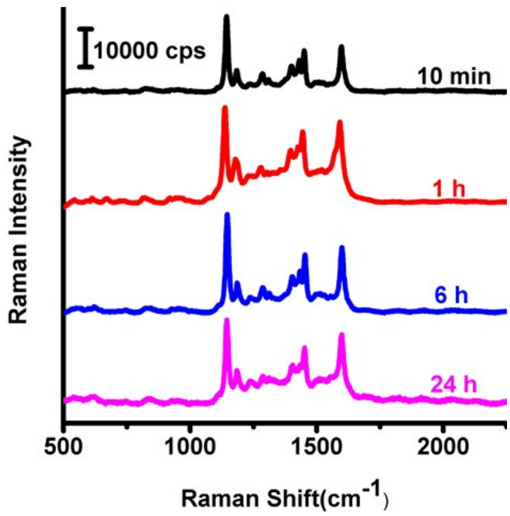

Figure S14. SERS spectra of benzidine molecules of different concentrations on the film of 25 nm AuAg ANPs coated on glass substrate in an artificial industrial wastewater (2 wt % NaCl, 1 mM H_2O_2, pH 10). The concentration of benzidine was varied from 5×10^{-7} M to 5×10^{-11} M. The excitation laser wavelength for Raman measurements is 633 nm and the acquisition time is 2 s.

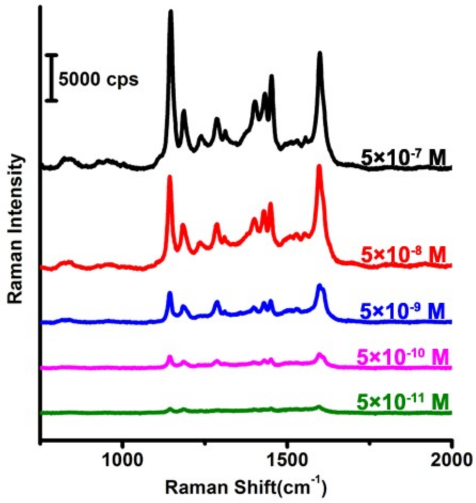

Figure S15. SERS spectra of p-Cresol (10 μM) in artificial industrial wastewater (2 wt % NaCl, 1 mM H_2O_2, pH 10) absorbed on the films of 25 nm AuAg ANCs (a) and 25 nm pure Ag NCs (b) cast on the glass substrates after incubation of substrates in the artificial industrial wastewater for 10 min (black curve) and 60 min (red curve). The excitation laser wavelength for Raman measurements is 633 nm and the acquisition time is 5 s.

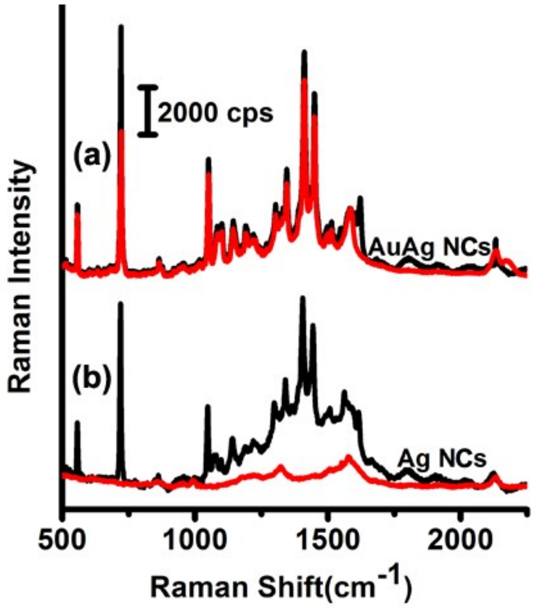

Table S1. Summarized table of SERS studies and performance of Ag NC-based and Au NC-based substrates.

	Shape	Size	Probe molecule	Detection concentration	EF	Excitation wavelength	Reference
Au NCs	nanospheres	24 nm	R6G	10^{-6} M	1.1×10^5	488 nm	[1]
	nanorods	15×75 nm			2.2×10^5		
	nanowires	15×650 nm			3.45×10^5		
	nanoprisms	65 nm			4.73×10^5		
	nanowires	12-80 nm	R6G	10^{-6} M	10^6	365 nm	[2]
	nanoparticles	50/69 nm	isocarbophos	N/A	N/A	780 nm	[3]
Ag NCs	nanospheres	11-23 nm	methylene blue	10^{-10} M	N/A	633 nm	[4]
	nanocubes	39.2 nm	1,4-BDT	10^{-9} M	3.1×10^5	785 nm	[5]
	wirelike	17 nm	MB	10^{-12} M	10^{10}	488 nm	[6]
	nanosheets	70 nm	4-MBA	10^{-12} M	N/A	785 nm	[7]
AgAu ANCs	nanocubes	50.5 nm	1,4-BDT	10^{-10} M	10^7	785 nm	[5]

Table S2. Comparison of SERS performance between Ag NCs and Au NCs with similar size and shapes.

Shape	Size	SERS performance	References
Nanospheres	22 nm	Au/Ag alloyed NPs ≈ Au@Ag NPs >> Ag NPs >> Au NPs	[8]
Nanospheres	61 nm	porous Au−Ag alloy nanoparticles >> Au NPs	[9]
Nanocubes	39.2 nm	Ag–Au hollow nanocubes > Ag–Au nanoboxes > Ag nanocubes	[5]
Nanorods	12.6×55 nm	AuNR@AuAg NRs ≈ AuNR@Au@Ag NRs ≈ AuNR@Ag NRs >> AuNR@Au NRs	[10]

Table S3. Comparison of chemical stability in SERS applications between Ag NCs and Au NCs as substrates.

Shape	Dimension	Chemical stability in SERS	Reference
Nanospheres	22 nm	Au/Ag alloyed NPs (44 h) ≈ Au NPs >> Au@Ag NPs ≈ Ag NPs (1 second)	[8]
Nanocubes	39.2 nm	Ag–Au hollow nanocubes (4 h) >> Ag nanocubes (5 min)	[5]
Nanorods	12.6×55 nm	AuNR@AuAg NRs >> AuNR@Au@Ag NRs ≈ AuNR@Ag NRs ≈ AuNR@Au NRs	[10]
Truncated triangular Nanoplates	9×55 nm	Ag@Au core/shell nanoplates (48 h)>> Ag nanoplates (30 min)	[11]

Table S4. Summary of size, particle number concentration and Ag amount of AuAg ANCs and CS AuAg ANCs used for SRES measurements.[a]

Types of NCs	AuAg ANCs			CS AuAg ANCs			
Diameter (nm)	11	16	25	30	46	64	80
particle number concentration (nM)	170.2	65.5	16.8	30.2	4.6	1.7	0.9
Ag amount (nM)	3.3	3.3	3.3	8.9	8.9	8.9	8.9

[a]Note that in each group, the total Ag amount is same while the particle number concentrations are different due to size effect. Moreover, the proper Ag amount in each group was selected for stable SERS measurements.

Table S5. Summarized data of Au ratios and Ag ratios from the center to outer part of 25 nm AuAg ANCs obtained from point-by-point STEM-EDS.

25 nm AuAg ANCs	Point 1	Point 2	Point 3	Point 4
Atomic percent of Au / %	73	69	65	60
Atomic percent of Ag / %	27	31	35	40

Table S6. Summarized data of Au ratios and Ag ratios from the center to outer part of 46 nm CS AuAg ANCs obtained from point-by-point STEM-EDS.

46 nm CS AuAg ANCs	Point 1	Point 2	Point 3	Point 4
Atomic percent of Au / %	57	48	25	10
Atomic percent of Ag / %	43	52	75	90

Table S7. Summarized data of Au ratios and Ag ratios from the center to outer part of 80 nm CS AuAg ANCs obtained from point-by-point STEM-EDS.

80 nm CS AuAg ANCs	Point 1	Point 2	Point 3	Point 4
Atomic percent of Au / %	53	43	26	9
Atomic percent of Ag / %	47	57	74	91

Table S8. Summarized data of intermediate products of 25 nm AuAg ANCs extracted at different reaction time.

Number	a	b	c	d	e	f	g	h	i	j	k
Reaction time /s	10	20	30	60	120	180	240	300	360	480	600
Size /nm	7.4±3	8.2±2	9.0±2	10.4±2	---	16.1±3	---	18.67±4	---	---	21.08±3
SPR band /nm	515.5	513.2	507.2	496.6	493.1	487.1	481.3	477.7	468.2	465.9	446.9
Atomic percent of Au / %	86	83	80	76	---	73	---	63	---	---	61
Atomic percent of Ag / %	14	17	20	24	---	27	---	37	---	---	39

Table S9. Summarized data of final compositions of AuAg ANCs with sizes of 11 to 25 nm and CS AuAg ANCs with sizes of 30 to 80 nm.

Sample image	1a	1b	1c	1d	2a	2b	2c	2d
Size /nm	10	11	16	25	30	46	64	80
Additional ratio of Ag^{+}/Au^{3+}	0	0.68	1.36	1.36	2.72	6.8	6.8	6.8
Ratio of Ag^{+}/Au^{3+} in samples	0	0.17	0.45	0.49	1.38	1.63	2.57	2.85

Reference:

[1] S. Kundu, *J. Mater. Chem. C*, 2013, **1**, 831–842.

[2] S. Kundu and M. Jayachandran, *RSC Adv.*, 2013, **3**, 16486–16498.

[3] R. Y. Hou, S. Panga and L. L. He, *Anal. Methods*, 2015, **7**, 6325–6330.

[4] O. Olea-Mejíaa, M. Fernández-Mondragóna, G. Rodríguez-de la Conchaa and M. Camacho-López, *Appl. Surf. Sci.*, 2015, **348**, 66-70.

[5] J. M. Li, Y. Yang and D. Qin. *J. Mater. Chem. C*, 2014, **2**, 9934–9940.

[6] D. Majumdar, A. Singha, P. K. Mondal and S. Kundu, *ACS Appl. Mater. Interfaces*, 2013, **5**, 7798−7807.

[7] J. Yan, X. J. Han, J. J. He, L. L. Kang, B. Zhang, Y. C. Du, H. T. Zhao, Cunku Dong, H. L. Wang and P. Xu, *ACS Appl. Mater. Interfaces*, 2012, **4**, 2752−2756.

[8] C. B. Gao, Y. X. Hu, M. S. Wang, M. F. Chi and Y. D. Yin, *J. Am. Chem. Soc.*, 2014, **136**, 7474–7479.

[9] K. Liu, Y. C. Bai, L. Zhang, Z. B. Yang, Q. K. Fan, H. Q. Zheng, Y. D. Yin and C. B. Gao, *Nano lett.*, 2016, DOI: 10.1021/acs.nanolett.6b00868

[10] J. F. Huang, Y. H. Zhu, C. X. Liu, Y. F. Zhao, Z. H. Liu, M. N. Hedhili, A. Fratalocchi and Y. Han, *Small*, 2015, **11**, 5214–5221.

[11] H. P. Liu, T. Z. Liu, L. Zhang, L. Han, C. B. Gao and Y. D. Yin, *Adv. Funct. Mater.* 2015, **25**, 5435–5443.